



Multiple CheY Proteins Control Surface-Associated Lifestyles of *Azospirillum brasilense*

Elena E. Ganusova, Lam T. Vo, Tanmoy Mukherjee[†] and Gladys Alexandre^{*}

Department of Biochemistry and Cellular and Molecular Biology, University of Tennessee, Knoxville, TN, United States

OPEN ACCESS

Edited by:

Seiji Kojima,
Nagoya University, Japan

Reviewed by:

Shuichi Nakamura,
Tohoku University, Japan
Kai Thormann,
University of Giessen, Germany

*Correspondence:

Gladys Alexandre
galexan2@utk.edu

[†]Present address:

Tanmoy Mukherjee,
Nationwide Children's Hospital,
Columbus, OH, United States

Specialty section:

This article was submitted to
Microbial Physiology and Metabolism,
a section of the journal
Frontiers in Microbiology

Received: 06 February 2021

Accepted: 29 March 2021

Published: 22 April 2021

Citation:

Ganusova EE, Vo LT,
Mukherjee T and Alexandre G (2021)
Multiple CheY Proteins Control
Surface-Associated Lifestyles of
Azospirillum brasilense.
Front. Microbiol. 12:664826.
doi: 10.3389/fmicb.2021.664826

Bacterial chemotaxis is the directed movement of motile bacteria in gradients of chemoeffectors. This behavior is mediated by dedicated signal transduction pathways that couple environment sensing with changes in the direction of rotation of flagellar motors to ultimately affect the motility pattern. *Azospirillum brasilense* uses two distinct chemotaxis pathways, named Che1 and Che4, and four different response regulators (CheY1, CheY4, CheY6, and CheY7) to control the swimming pattern during chemotaxis. Each of the CheY homologs was shown to differentially affect the rotational bias of the polar flagellum and chemotaxis. The role, if any, of these CheY homologs in swarming, which depends on a distinct lateral flagella system or in attachment is not known. Here, we characterize CheY homologs' roles in swimming, swarming, and attachment to abiotic and biotic (wheat roots) surfaces and biofilm formation. We show that while strains lacking CheY1 and CheY6 are still able to navigate air gradients, strains lacking CheY4 and CheY7 are chemotaxis null. Expansion of swarming colonies in the presence of gradients requires chemotaxis. The induction of swarming depends on CheY4 and CheY7, but the cells' organization as dense clusters in productive swarms appear to depend on functional CheYs but not chemotaxis *per se*. Similarly, functional CheY homologs but not chemotaxis, contribute to attachment to both abiotic and root surfaces as well as to biofilm formation, although these effects are likely dependent on additional cell surface properties such as adhesiveness. Collectively, our data highlight distinct roles for multiple CheY homologs and for chemotaxis on swarming and attachment to surfaces.

Keywords: *Azospirillum*, CheY, chemotaxis, flagella, swarming, surface attachment

INTRODUCTION

Navigating chemical gradients requires motile bacteria to sense and bias their direction of movement using chemotaxis. Motile and flagellated bacteria utilize conserved and dedicated chemotaxis signal transduction pathways to modulate swimming bias in chemical gradients. In *Escherichia coli*, the chemotaxis system comprises a single set of membrane-bound chemoreceptors, chemotaxis histidine kinase (CheA), flagellar-motor binding response regulator (CheY), and scaffolding protein (CheW). Adaptation proteins methylesterase CheB and methyltransferase CheR re-set signaling upon excitation by reversibly modifying membrane-bound chemoreceptors (Levit and Stock, 2002). The majority of motile, flagellated bacterial

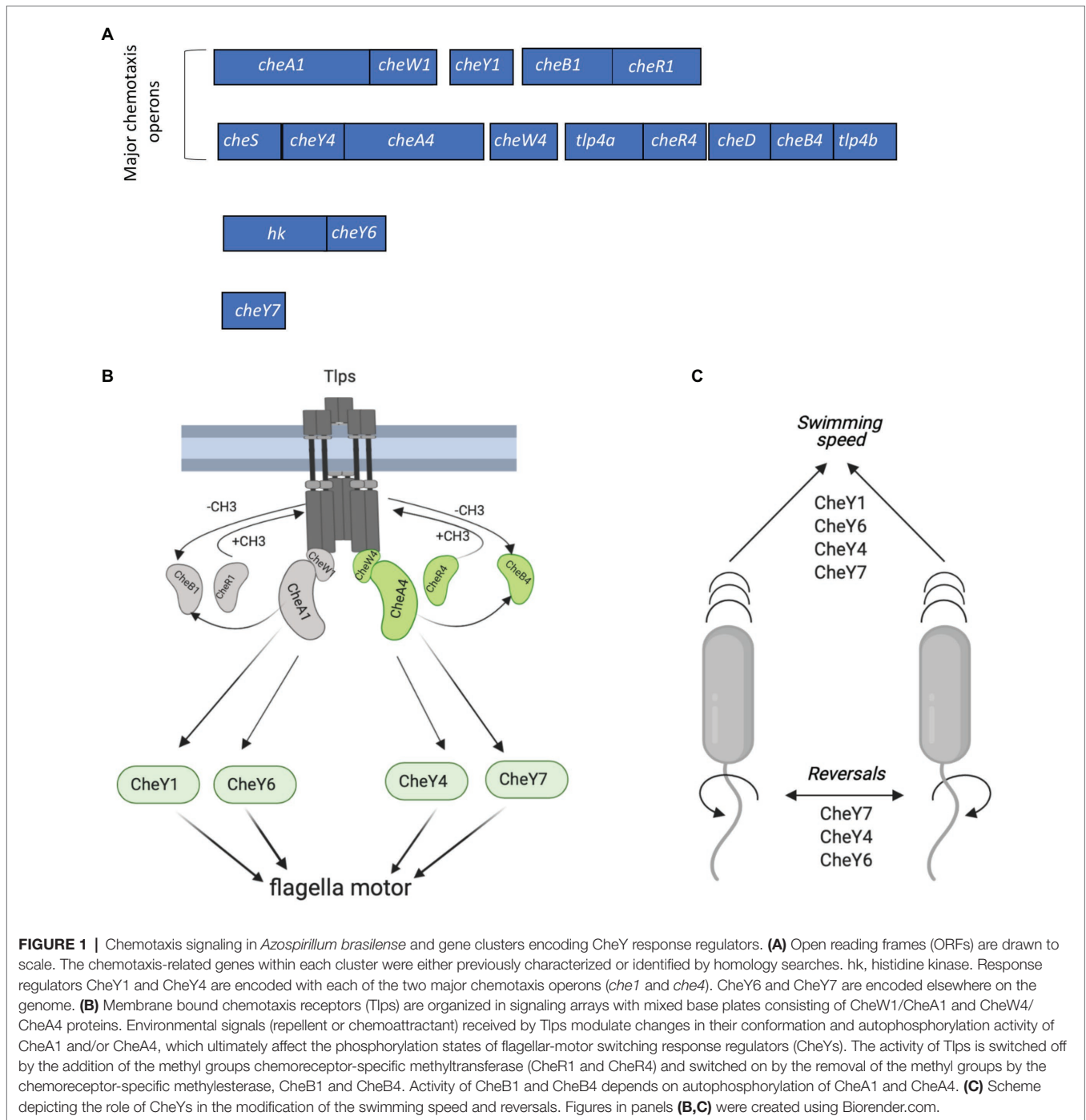
sequenced genomes indicates the presence of multiple chemotaxis as well as chemosensory (chemotaxis-like) pathways, with the latter displaying non-motility phenotypes such as extracellular matrix formation (Edwards et al., 2011), cyst formation (Berleman and Bauer, 2005; Wu et al., 2011), biofilm formation (Huang et al., 2019), and quorum sensing (Laganenka et al., 2016). In contrast to *E. coli* which possesses a single chemotaxis response regulator CheY to alter the direction of rotation of flagellar motors, the genome of many bacteria encodes for multiple CheY homologs: *Rhodobacter sphaeroides* (Ferré et al., 2004; Porter et al., 2006), *Sinorhizobium meliloti* (Schmitt, 2002), *Rhizobium leguminosarum* (Miller et al., 2007), *Azospirillum brasilense* (Mukherjee et al., 2016, 2019), *Borrelia burgdorferi* (Pitzer et al., 2011), *Vibrio cholerae* (Hyakutake et al., 2005), etc. In some cases, the multiple CheY homologs are encoded within a single chemotaxis pathway (e.g., *S. meliloti*). These CheYs may also be encoded elsewhere on the genome with no apparent genetic link to a particular chemotaxis system (e.g., *B. burgdorferi*; Schmitt, 2002; Pitzer et al., 2011). Why motile bacteria have multiple chemotaxis-related response regulators is not clear. In *R. sphaeroides*, all six CheY homologs are able to bind to the FliM component of the flagellar motor upon phosphorylation, but only one of them is responsible for the flagella motor stopping (Ferré et al., 2004).

The alphaproteobacterium *A. brasilense* are soil motile diazotrophic bacteria able to colonize the roots of diverse plants and promote their growth through phytohormones production and nitrogen fixation (Steenhoudt and Vanderleyden, 2000). *A. brasilense* motility and chemotaxis are important for plant root colonization (Zhulin and Armitage, 1992; Greer-Phillips et al., 2004; O'Neal et al., 2019, 2020). *A. brasilense* cells are motile using a single polar flagellum that allows the cells to swim in liquid media and when the viscosity of the media increases, cells produce multiple lateral flagella, structurally distinct from the polar flagellum, that permit translocation across surfaces by swarming (Moens et al., 1996). The polar flagellum of *A. brasilense* cells rotates in both clockwise and counterclockwise directions, and chemotaxis signaling controls the rotational bias of the polar flagellum in this species (Zhulin and Armitage, 1993; Mukherjee et al., 2019). The *A. brasilense* polar flagellum is comprised of flagellin that is glycosylated (Moens et al., 1995b). The glycosylation on the *A. brasilense* polar flagellin consists of a branched tetrasaccharide with repeated rhamnose, fucose, galactose, and *N*-acetylglucosamine that resemble the LPS O-antigen, suggesting that both structures are related (Belyakov et al., 2012). The polar flagellum was suggested to mediate adsorption of *A. brasilense* cells to the roots of wheat plants in a two-step attachment process (Croes et al., 1993): a reversible step that is thought to be mediated by the polar flagellum and an irreversible attachment step that likely involves extracellular polymeric substances. The *A. brasilense* polar flagellum also contributes to biofilm formation *in vitro* and to the stabilization of the biofilm matrix (Viruega-Góngora et al., 2020). The lateral flagella required for swarming are distinct appendages made of proteins unrelated to the polar flagellum, including distinct lateral flagellin, termed Laf1 (Moens et al., 1995a). Lateral flagella are produced when the rotation of the polar flagellum is hindered

(Moens et al., 1996), and recent evidence indicates that an extracytoplasmic function (ECF) sigma-factor ultimately regulates lateral flagellar biosynthesis in *A. brasilense* (Dubey et al., 2020).

Chemotaxis in *A. brasilense* controls the polar flagellum and thus swimming through signaling *via* two different chemotaxis systems, named Che1 and Che4, as well as additional CheY response regulators (CheY6 and CheY7) encoded outside of *che1* and *che4* (Bible et al., 2012; Mukherjee et al., 2016, 2019; **Figure 1A**). Histidine kinase CheA1 and the response regulator CheY1, both encoded within the *che1* cluster, regulate transient changes in swimming speed during chemotaxis. CheA4 histidine kinase and the CheY4 response regulator, both encoded within the *che4* operon, control the probability of changes in the swimming direction (herein reversals) during chemotaxis (**Figure 1B**). A $\Delta cheY6$ mutant has a swimming reversal phenotype similar to that of a $\Delta cheY4$ mutant, while a strain lacking CheY7 does not display any swimming reversals. All CheY mutants also swim slower than the wild type in the absence of a gradient (**Figure 1C**; Mukherjee et al., 2019). Genetic evidence and behavioral assays indicate that CheY6 activity is controlled by Che1/CheA1 signaling, and CheY7 activity, a mutant of which phenocopies a $\Delta cheA4$ mutant, is controlled by Che4/CheA4 signaling (Mukherjee et al., 2019; **Figure 1A**). Mutants lacking *cheA4*, *cheY4*, or *cheY7* are unable of chemotaxis in spatial gradients of chemoeffectors, while mutants lacking *cheY1* or *cheY6* still display chemotaxis under these conditions (Bible et al., 2008; Mukherjee et al., 2016, 2019). Another feature of the polar flagellum motor of *A. brasilense* is that it undergoes brief swimming pauses, which are distinct from speed increases or reversals. Swimming pause frequency is reduced in strains lacking CheY1, CheY6, and CheY7 but is increased in a strain lacking CheY4, although the mechanism for these differential effects is not known (**Figure 1B**; Mukherjee et al., 2019). The effects of these CheY homologs on the swimming motility pattern of *A. brasilense* are thought to optimize navigation in the spatially and physically heterogeneous environment of the soil, although this remains to be experimentally demonstrated.

Rotation (or lack thereof) of flagella controlling swimming motility has been implicated in the swim-to-sessile transitions in diverse bacteria, perhaps through the flagellum acting as a “mechanosensor” (Gordon and Wang, 2019; Chawla et al., 2020). Such swim-to-sessile transitions occur during swarming on surfaces, the formation of biofilms, and surface attachment (Guttenplan and Kearns, 2013). Chemotaxis and chemotaxis mutants with different motility biases have been implicated in bacterial social behaviors, promoting cell-to-cell interactions or interaction with eukaryotic hosts (Alexandre, 2015). However, the exact role of the rotational bias of flagella or multiple chemotaxis CheY homologs in these behaviors has been seldom, if at all, addressed. Here, we take advantage of the different effects of *A. brasilense* CheYs (CheY1, CheY4, CheY6, and CheY7) on the rotational bias of the polar flagellum and chemotaxis to examine contributions to behaviors related to swim-to-stick transitions such as swarming, surface (abiotic and wheat) attachment, and biofilm formation. We show that only some of these CheYs (CheY4 and CheY7) but not chemotaxis *per se* induce swarming, and CheYs mediate distinct abiotic



surfaces and wheat roots attachment as well as biofilm formation. Together, the findings indicate that CheY homologs contribute to distinct swim-to-stick behaviors.

MATERIALS AND METHODS

Bacterial Strains and Culture Conditions

The bacterial strains used in this study are listed in **Table 1**. *A. brasilense* strains were cultured in the minimal medium

(MMAB; Hauwaerts et al., 2002) or TY (tryptone 10 g/L, yeast extract 5 g/L; Bible et al., 2012); and washed in a chemotaxis buffer [10 mM phosphate buffer (pH 7.0), 1 mM EDTA] as described previously (Stephens et al., 2006). Conjugation was performed on D-plates (8 g/L Bacto Nutrient broth, 0.25 g/L MgSO₄ 7H₂O, 1.0 g/L KCl, 0.01 g/L MnCl₂, 2% agar) and, after conjugation, MMAB with appropriate antibiotics was used for selection of *A. brasilense* transconjugants. The *A. brasilense* wild type (Sp7), mutant strains, and complemented derivatives were grown at 28°C, with shaking. Unless otherwise stated,

TABLE 1 | The list of strains and plasmid used in this study.

Strain or plasmid	Description	Reference or source
<i>A. brasilense</i> Sp7	Wild type strain	ATCC 29145
$\Delta cheY1$	$\Delta cheY1::Km$ (Km ^r)	Bible et al., 2008
$\Delta cheY4$	$\Delta cheY4::Cm$ (Cm ^r)	Mukherjee et al., 2016
$\Delta cheY7$	$\Delta cheY7::Gm$ (Gm ^r)	Mukherjee et al., 2019
$\Delta cheY6$	$\Delta cheY6$, markerless	Mukherjee et al., 2019
$rpoN::Km^r$	$rpoN::Kmr$ in Sp7 (Km ^r)	Milcamps et al., 1996
<i>E. coli</i>	General cloning	Invitrogen™
TOP10	F- <i>mcrA</i> $\Delta(mrr-hsdRMS-mcrBC)$ $\phi 80lacZ\Delta M15$ $\Delta lacX74$ <i>recA1</i> <i>araD139</i> $\Delta(araleu)7697$ <i>galU</i> <i>galK</i> λ^{-} <i>rpsL</i> (Str ^r) <i>endA1</i> <i>nupG</i>	Simon et al., 1983
pRK2013	Helper plasmid for triparental mating (ColE1 replicon, Tra, Km ^r)	Figurski and Helinski, 1979
pHRGFP	pBBR1 origin plasmid expressing GFP (Tc ^r)	Ramos et al., 2002
pRH005	Gateway-based destination vector expressing proteins fused with YFP at the C-terminus, Km ^r , Cm ^r	Hallez et al., 2007
pRHCheY4	pRH005 plasmid with CheY4 ORF fused with YFP at the C-terminus (CheY4-YFP)	O'Neal et al., 2019
pRHCheY7	pRH005 plasmid with CheY7 ORF fused with YFP at the C-terminus (CheY7-YFP)	this study
pRK415	Broad host range vector (Tc ^r)	Keen et al., 1988
pRKCheY1	pRK415 containing <i>cheY1</i> (Tc ^r)	Bible et al., 2008
pRKCheY4	pRK415 containing <i>cheY4</i> (Tc ^r)	Mukherjee et al., 2016
pRKCheY6	pRK415 containing <i>cheY6</i> (Tc ^r)	Mukherjee et al., 2019
pRKCheY7	pRK415 containing <i>cheY7</i> (Tc ^r)	Mukherjee et al., 2019

the antibiotics were used at the following concentrations: 200 µg/ml ampicillin, 30 µg/ml kanamycin (Km), 20 µg/ml gentamicin (Gm), 34 µg/ml chloramphenicol (Cm), and tetracycline (Tc) 5 µg/ml. CheY7-YFP complementation construct was obtained using Gateway cloning (Invitrogen) and the pRH005 vector according to the published protocols (Hallez et al., 2007). *cheY7* gene was amplified using Gateway primers (Table 1) and Sp7 *A. brasilense* genomic DNA as a template. Five microliters of PCR product were run on a 0.8% gel for verification of the insert, and PCR cleanup (Nucleospin Gel and PCR cleanup, Macherey-Nagel™) was performed on the remainder of the PCR product. The resulting PCR product was used for a BP Clonase (Invitrogen™) reaction with the pDONR2.1 vector (Invitrogen™). This reaction was then transformed into *E. coli* Top10 chemically competent cells and plated on Luria broth (LB, 10 g/l tryptone, 5 g/l yeast extract, 10 g/l NaCl) with 50 mg/ml kanamycin. Colonies from these plates were grown in 5 ml of LB with kanamycin (50 µg/ml) and subjected to plasmid purification (Qiagen™). The resulting plasmids were used for the LR Gateway reaction (in the Gateway cloning

LR Reaction stands for a recombination reaction between attL and attR sites; Invitrogen™) with the pRH005 plasmid.

Chemotaxis, Swimming, and Swarming Behavioral Assays

For the aerotaxis spatial gradient assay, free-swimming cells from exponentially grown cultures were washed twice with chemotaxis buffer and placed in a 1 mm flat capillary tube (inner dimensions, 0.1 by 2 by 50 mm; VitroCom, Mountain Lakes, NJ, United States). The formation of a band of motile bacteria near the air-liquid interface was observed at 60 s post-introduction into the capillary tube, and the distance between the meniscus and the band was measured. Aerotaxis band formation was recorded using a Nikon microscope with a Nikon Coolpix mounted camera.

For the swimming and swarming assays in Petri plates, a single colony from each strain was inoculated in 5 ml of MMAB medium and grown until OD₆₀₀ = 0.8. The culture was then washed once with modified chemotaxis buffer [10 mM phosphate buffer (pH 7.0)], and 5 µl of the culture was placed on top of 13 g/l Nutrient broth (Fisher Scientific™) solidified with 0.2, 0.3, 0.4, 0.5 0.6, or 0.7% (w/vol) of noble agar (Fisher Scientific™). A swarming time-course assay was conducted using 0.6% noble agar added to MMAB and supplemented with 0.5% Tween-20 since preliminary data indicated its addition promoted reproducible and robust swarming (Wu et al., 2020). The plates were incubated at 28°C for 24–96 h, and the diameter of the expansion rings was measured.

To observe the development of swarming colonies under the microscope, we used the pHRGFP plasmid with constitutive green fluorescent protein (GFP) expression in *A. brasilense* (Ramos et al., 2002). The pHRGFP plasmid was introduced into the wild type Sp7 strain and its *cheY* mutant derivatives by conjugation. Three hundred microliters of the swarming medium [MMAB with 0.6% (w/v) noble agar and supplemented with 0.5% Tween-20] were placed in the well of an EISCO Concavity Microscope slide (Fischer Scientific™). Two microliters of the cell culture, prepared as for the swarm plates assay above, were diluted to an OD₆₀₀ = 0.8 and placed at the center of the swarming medium. Under these conditions, swarming of the cells was observed using a GFP filter, 4x objective mounted to a Nikon ECLIPSE 80i fluorescence microscope with a Nikon CoolSnap HQ2-cooled charge-coupled device (CCD) camera and photographed in 2, 6, and 24 h. The experiment was conducted in triplicate. Whole colony swarming fluorescence images were obtained using a Leica MZI67A dissecting scope equipped with a GFP fluorescence filter. Leica application suite software was used for the image collection. To observe the formation of cell clusters in swarming colonies of *A. brasilense* Sp7 and a *rpoN::Km^r* harboring a pHRGFP plasmid, slides were prepared the same way as described above except a cover slip was placed on the top of the agar inoculated with cells. Clusters were observed using a GFP filter, 100x objective mounted to a Nikon ECLIPSE 80i fluorescence microscope with a Nikon CoolSnap HQ2-cooled charge-coupled device (CCD) camera and photographed at 2, 6, and 24 h post inoculation.

Flagella Staining

Flagella staining was performed on cells grown in liquid medium (swimming) or collected from swimming/swarming MMAB media made with 0.2–0.7% (w/vol) agar plates after 48 h incubation and stained using Alexa Fluor™ 488 NHS Ester (Succinimidyl Ester; Fisher Scientific™) as described in (Gunsolus et al., 2014) with slight modifications. Briefly, cells were resuspended in 75 µl of phosphate buffer saline (PBS; 137 mM NaCl, 2.7 mM KCl, 10 mM Na₂HPO₄, 1.8 mM KH₂PO₄) supplemented with 1 mM EDTA and 0.5% Brij™-35 detergent (Fisher Scientific™) to avoid cell-to-cell adhesion at OD₆₀₀ = 1 and 25 µl of 1 M sodium bicarbonate bicarbonate buffer was added to the cell suspension to stabilize the pH. A 1 µl of 0.5 mg ml⁻¹ Alexa Fluor 488 carboxylic acid succinimidyl ester (Fisher Scientific™) in DMSO (Sigma Aldrich) was added. The resulting suspension was incubated in the dark for 1 h at room temperature with frequent mixing. The suspension was then centrifuged at 4,000 rpm for 3 min, the supernatant was discarded, and the cell pellet was washed with 500 µl of PBS. Cells were mounted on an agar pad (1% low melting point agarose in PBS) and covered with a glass coverslip, and left on the bench for 10 min. Images were taken using a 63x objective with oil immersion mounted to a Leica SP8 with White Light Laser Confocal System; Leica, Wetzlar, Germany). Images were collected using a 488-nm excitation Argon ion laser with an emission maximum at 517 nm.

Measurements of Cell Size

Cells were washed once with PBS buffer and resuspended in TBAC buffer [PBS containing 1 mM EDTA and 0.01% (v/v) Tween 20] to avoid the formation of bacterial aggregates (Alves et al., 2017). Cell sizes were measured using the Prism 8 program for a minimum of 60–100 cells per sample taken from at least four different fields of view. Confocal microscopy (Leica SP8 White Light Laser Confocal System) images were taken at random fields of view. Several images were collected for each experiment. For cell length measurements, all cells within the field of view were measured from one cell pole to the other at the longest axis.

Western Blotting, Coomassie Staining, and Flagella Glycosylation Staining

For isolation of polar flagella, each strain was grown to the mid-log phase (OD₆₀₀ = 0.7–0.8) in liquid MMAB. Cells were pelleted for 3 min at 4,600 rpm using a tabletop Eppendorf centrifuge and washed once with 1 ml of PBS buffer. The resulting pellet was resuspended in 150 µl of 1x Laemmli buffer (4% SDS, 10% beta-mercaptoethanol, 20% glycerol, 0.1 M Tris pH 6.8, and 0.005% of bromophenol blue) in PBS. Cells were vigorously vortexed for 1 min and spun down for 15 min at 4°C and 13,000 rpm using a tabletop Eppendorf centrifuge. The supernatant was collected and heated for 5 min at 65°C to denature proteins. For isolation of lateral flagella, each strain was grown on the top of the swarming medium (MMAB supplemented with 0.6% of noble agar and 0.5% of Tween-20) for 48 h at 28°C. Cells were then scraped from the plate and

resuspended in PBS. Flagella isolation was done as described for the isolation of polar flagella. Twenty microliters of isolated flagellins were loaded on SDS-PAGE gels (8% resolving gel for polar flagellin analysis and 12% resolving gel for lateral flagellin detection). Mini-Protean gel system was used for protein separation (Bio-Rad™). The gel ran at 120 V for 90 min. The gel was then transferred to a 0.45 µm hydrophobic polyvinylidene difluoride (PVDF) transfer membrane (Immobilon) using a wet transfer apparatus (Bio-Rad). The transfer ran at 90 V for 1 h and 10 min. The membrane was blotted for 40 min in 5% milk in Tris-buffered saline (TBS; 6.05 g/L Tris, 8.76 g/L NaCl, pH 7.5) supplemented with Tween-20 (0.1%; TBST). After blocking, the membrane was incubated with primary polyclonal anti-polar and anti-lateral flagellin antisera (Alexandre et al., 1999) in TBST at 1:1,000 for 16 h at 4°C with agitation. The membrane was washed twice with 5% milk in TBST, twice in TBST, and twice in TBS. The membrane was then incubated with secondary anti-rabbit antibodies, diluted to 1:10,000 in TBS for 1 h, and washed again with the solutions mentioned above. Lateral protein production was quantitated using Fiji ImageJ (NIH). Coomassie blue dye (2 g/L of water) was used to monitor total proteins loaded. SDS-PAGE gels were de-stained using a mix of H₂O, methanol, and acetic acid detected using the Glycoprotein Staining Kit (Thermo Scientific™ Pierce™) according to the manufacturer's manual. Briefly, *A. brasilense* cells were grown in flasks with 25 ml of MMAB medium with shaking at 175 rpm, at 28°C. Cell cultures were spun down at 3,000 rpm in a 50-ml Falcon tube, cell pellets were washed once with PBS, and flagella were sheared for 1 min using a vortex, resuspended in 20 ml of PBS, kept on ice for 5 min, and spun down at 22,000 rpm using a Beckman ultracentrifuge with a T70i fixed-angle titanium rotor for 90 min. The pellets were resuspended in 200 µl of 1x Laemmli buffer in PBS. Samples were heated for 5 min at 60°C before loading onto an 8% SDS-PAGE gel.

Abiotic Surface Attachment Assay

For the abiotic surface attachment assay, *A. brasilense* Sp7 strain and its *cheY* mutant derivatives carrying the pHRGFP plasmid (Ramos et al., 2002) were cultured overnight in TY medium supplemented with tetracycline for plasmid maintenance. Cells were washed with a chemotaxis buffer and resuspended in the chemotaxis buffer to a final OD₆₀₀ = 0.4. Economy Plain Glass Microscope Slides Glass slides (Fisher Scientific™) were covered with 0.01% poly-lysine (Sigma™) and left to dry for 15 min. Ten microliters of cell cultures were placed on the slide and kept in a humidity chamber (square Petri dishes lined up with Kim Wipes wetted with sterile water) to prevent buffer evaporation. Cells remaining on the slide were washed with chemotaxis buffer 2 h after inoculation and imaged using a GFP filter, 4x objective mounted to a Nikon ECLIPSE 80i fluorescence microscope with a Nikon CoolSnap HQ2-cooled charge-coupled device (CCD) camera.

Biofilm Formation

Biofilm assay was performed in modified MMAB medium modified to achieve a C:N ratio = 2 using fructose at 27.6

and 13.8 mM KNO₃ as N source (Arruebarrena Di Palma et al., 2013). Two hundred microliters per well were transferred to sterile, clear flat-bottom polystyrene 96-well plates (Corning™) and incubated without agitation for 96 h at 28°C. Biofilm formation was determined using crystal violet staining (Arruebarrena Di Palma et al., 2013). Briefly, 200 µl of 0.5% crystal violet was added to each well, followed by incubation 30 min at room temperature, and then washed carefully three times with tap water. Crystal violet remaining attached to the wells was extracted with 200 µl of 33% v/v acetic acid. The OD₅₉₀ of supernatants was determined using a microplate Absorbance Reader with Gen5 software (BioTek Instruments, Winooski, Vermont, United States). Data were normalized by total growth estimated by OD₆₀₀ measured on the planktonic culture.

Wheat Root Attachment Assay

Triticum aestivum cv. Jagger (wheat) seeds were utilized throughout this study. *T. aestivum* seeds were surface-sterilized 10 min with 90% ethanol and 20 min with a sterilization buffer containing 1% Triton X-100, 10% bleach and sterile water. After sterilization, seeds were planted into c (0.132 g/l CaCl₂, 0.12 g/l MgSO₄ 7H₂O, 0.1 g/l KH₂PO₄, 0.075 g/l Na₂HPO₄ 2H₂O, 5 mg/l Fe-citrate, and 0.07 mg/l each of MnCl₂ 4H₂O, CuSO₄ 5H₂O, ZnCl₂, H₃BO₃, and Na₂MoO₄ 2H₂O, adjusted to pH 7.5 before autoclaving; Zamudio and Bastarrachea, 1994; de Oliveira Pinheiro et al., 2002; Greer-Phillips et al., 2004) and placed in the dark for 48 h to germinate. Next, seedlings were placed in 250 ml Mason jars containing 50 ml of semi-solid (0.5% w/vol Noble agar) Fahraeus medium and allowed to grow with 8 h day/16 h dark at 22°C in the plant growth chamber at 90,000 lux or 1,670 µmol m⁻² s⁻¹. All assays were performed on germinated and surface-sterilized seedlings that were 7–10 days old.

For the root attachment assay, *A. brasilense* strains were cultured in MMAB liquid overnight (28°C, 200 rpm). The cultures were normalized to an OD₆₀₀ = 0.6 using sterile chemotaxis buffer and resuspended in 2 ml of Fahraeus medium in a 15 ml Falcon tube. Wheat seedling with cut-off leaves was placed inside the tube, and tubes were incubated either at room temperature for 2 h or with shaking on a Ferris wheel for 2 h. After incubation, roots were washed three times with sterile chemotaxis buffer, resuspended in 2 ml sterile chemotaxis buffer and sonicated for 10 s, using a cell dismembrator (Model 100; Fisher Scientific™, Waltham, MA, United States). CFU recovered from the inoculum or after detachment from roots were counted by plating serial dilutions on TY plates supplemented with ampicillin. The results were expressed as a root attachment index, calculated as CFU detached from roots/CFU in the initial culture normalized to the total fresh weight of roots in milligrams.

Statistical Analysis

We used Student *t*-test using GraphPad Prism (version 8) software (GraphPad Software Inc., San Diego, CA, United States) to compare the wild type and mutant phenotypes (swimming/

swarming behavior on the plates, band quantitation, western blotting flocculation, biofilm formation, and plant root attachment).

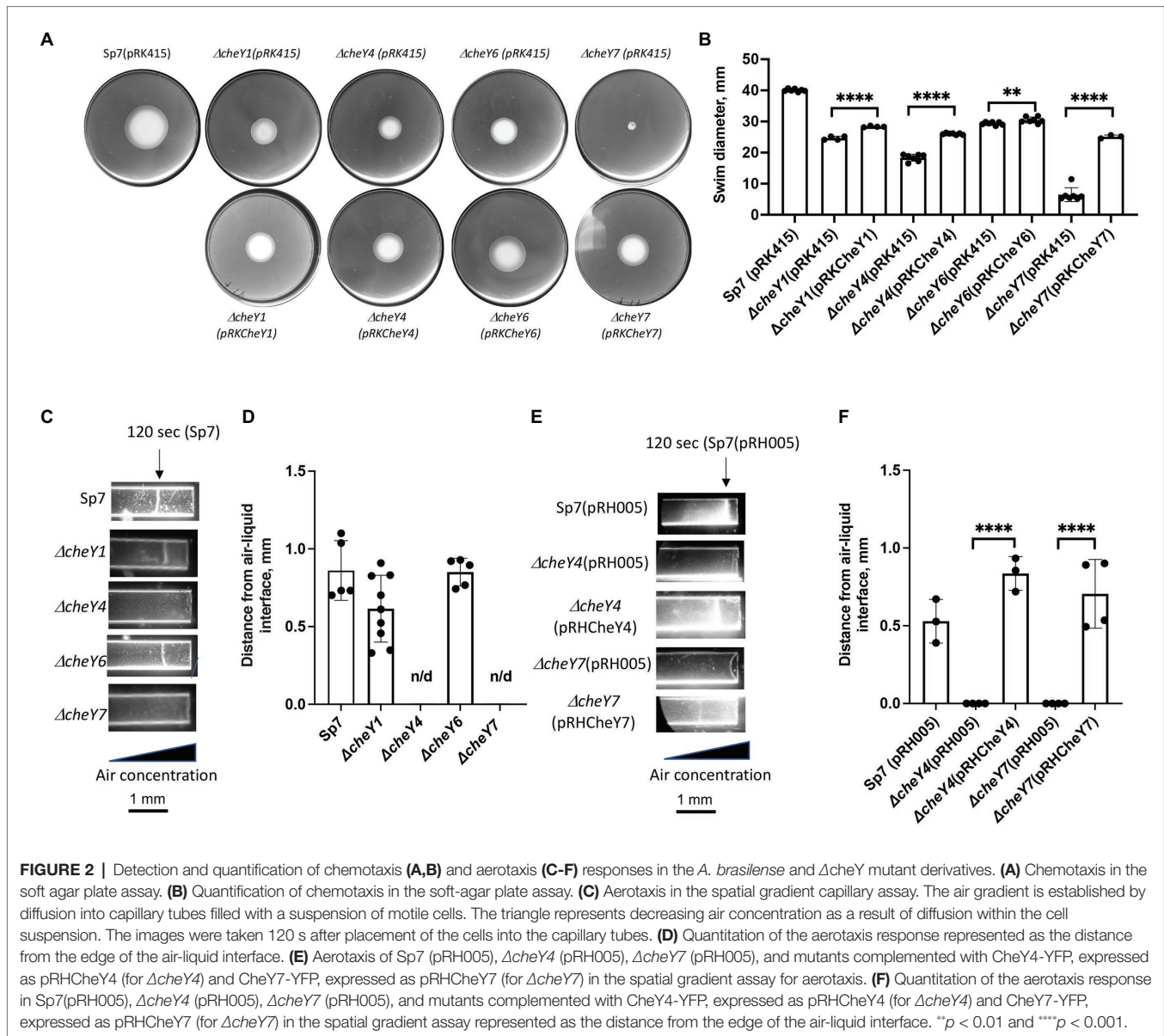
RESULTS

Azospirillum brasilense CheY6 and CheY7 Response Regulators Have Different Contributions to Aerotaxis

Our previous work has shown that minor ($\Delta cheY1$ and $\Delta cheY6$ mutants) and severe ($\Delta cheY4$ and $\Delta cheY7$ mutants) defect in chemotaxis of the mutant strains could be functionally rescued by expressing parental genes from broad host range vectors (Bible et al., 2008, 2012; Mukherjee et al., 2016, 2019). Here, we confirm these previous observations by analyzing chemotaxis in swim plate assays (Figure 2A). The $\Delta cheY1$, $\Delta cheY4$, $\Delta cheY6$, and $\Delta cheY7$ mutants had slight or major chemotaxis defects that were partially complemented by expressing parental genes expressed from broad host range plasmids (Figures 2A,B). Partial functional complementation from this type of plasmids was reported previously (Bible et al., 2008). We also performed the aerotaxis assay with the mutant strains. Aerotaxis is a particular form of chemotaxis in air gradients and is regulated by the same chemotaxis pathways. Aerotaxis depends on near-immediate responses to the air gradient (~1–2 min) instead of the several days for observing a response in chemotaxis spatial gradient assays. Aerotaxis thus provides a more direct evaluation of the ability of cells to navigate gradients. In the aerotaxis gradient assay, an open-ended capillary tube is filled with a suspension of motile *A. brasilense* cells. An air gradient is established through the diffusion of air from the atmosphere into the cell suspension (Zhulin et al., 1996; Alexandre et al., 2000). Under these conditions, motile and chemotaxis-competent *A. brasilense* cells form a tight band of motile cells at a location in the gradient that corresponds to maximal energy generation (Zhulin et al., 1996; Figures 2C–F). Chemotaxis defects of the different *cheY* mutant strains were also complemented by expressing parental genes from plasmids (Figures 2A,B,E,F).

The Absence of CheY7 Causes Defects in Polar Flagellin Molecular Weight but Not Swimming Motility

All of the mutants lacking CheY1, CheY4, CheY6, or CheY7 are motile in liquid media and, as expected, possess polar flagella (Figure 3A). We used polyclonal antisera raised against the polar flagellin and Western blots to compare levels of production of the polar flagellin in the wild type Sp7 and its *cheY* mutant derivatives (Figure 3B). As a negative control, we used a *rpoN::Km^r* mutant which lacks both polar and lateral flagella production (Milcamps et al., 1996; Figures 3A,B). As expected, the anti-polar flagellin antisera recognized a band at a predicted ~100 kDa in all but the $\Delta cheY7$ mutant. In this mutant, the band corresponding to the polar flagellin migrated with an apparent molecular weight of ~90 kDa. A second band at about 45–50 kDa was also observed in the $\Delta cheY6$ mutant. This molecular weight is much lower than

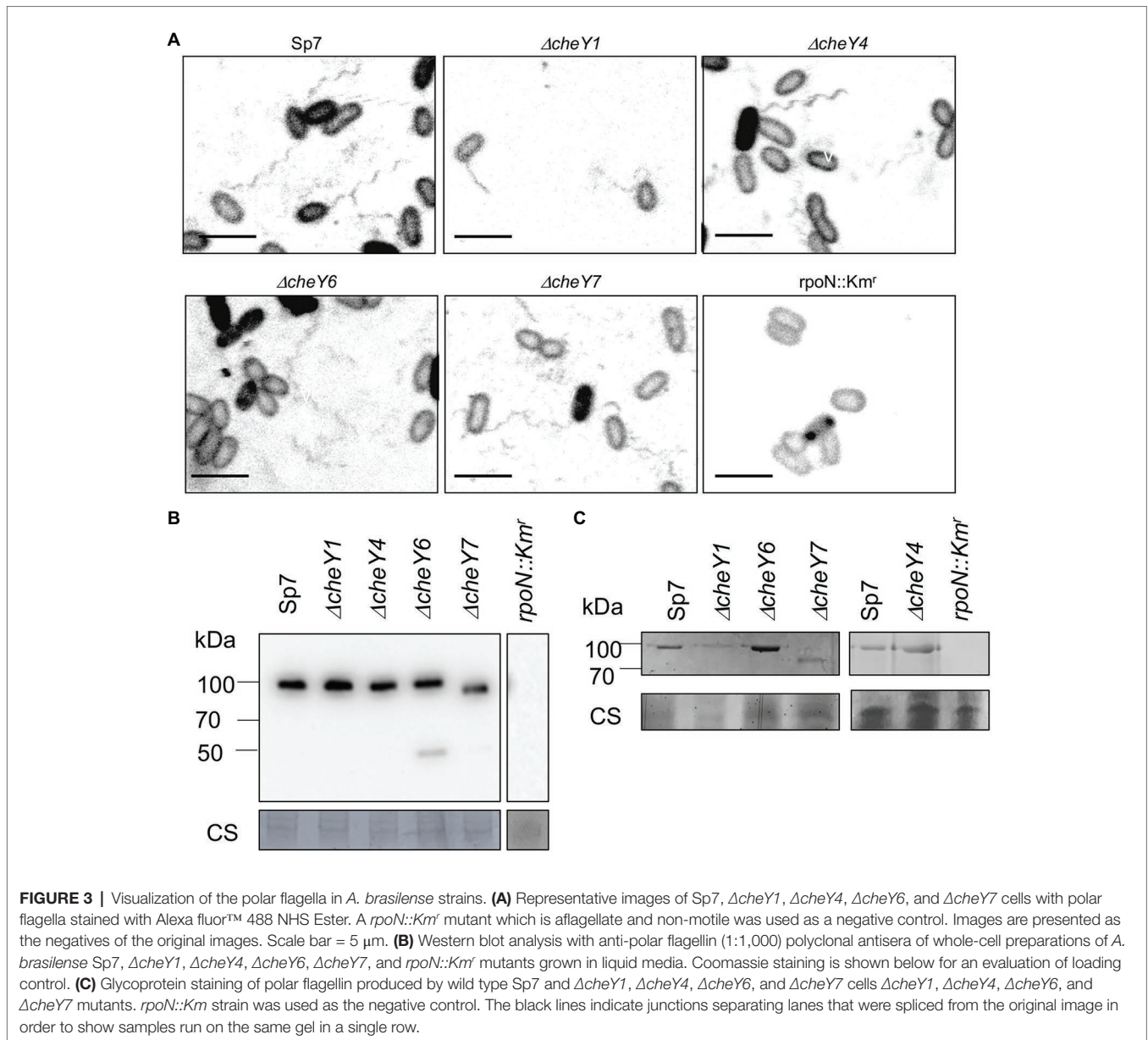


the predicted molecular weight for the two polar flagellins encoded in the *A. brasilense* genome (AMK58_10890 and AMK58-18185), which are expected to be about 65 kDa. The nature of this cross-reacting band is not known. The polar flagellin is glycosylated in *A. brasilense* and a fully glycosylated polar flagellin has a molecular weight of about 100 kDa, while complete chemical deglycosylation of the polar flagellin yields a band at ~65–70 kDa (Moens et al., 1995b). Therefore, we hypothesized that changes in the molecular weight of the polar flagellin in the $\Delta cheY7$ strain could result from reduced glycosylation of the polar flagellin. Analysis of glycosylated proteins from the same samples as those used for the Western blot above, identified a single band for a glycosylated protein at the same molecular weight as the polar flagellin for all strains except for the non-flagellated *rpoN::Km^r* strain (Figure 3C). Noticeably, a glycosylated band corresponding to

the polar flagellin of the $\Delta cheY7$ mutant was still present at a lower molecular weight (Figure 3C). The reduced molecular weight of the polar flagellin of the $\Delta cheY7$ mutant could suggest reduced glycosylation levels in this species. A $\Delta cheY7$ mutant is still fully motile, so this different glycosylation level has no apparent effect on polar flagellum function. This observation is intriguing because it suggests a functional link between CheY7 and polar flagellin maturation.

***Azospirillum brasilense* Chemotaxis CheY Homologs Contribute to Movement in Media of Varying Viscosity**

CheY homologs have different effects on the free-swimming motility pattern of *A. brasilense*: CheY1 affects the transient increase in swimming speed and has a minor impact on the probability of swimming reversals. In contrast, CheY4 and



CheY6 have severe defects in swimming reversals, and CheY7 cannot reverse the swimming direction (Mukherjee et al., 2019). These different effects are hypothesized to provide *A. brasilense* with swimming navigation strategies optimized for the heterogeneous physicochemical conditions found in the soil. Here, we probe the chemotaxis response regulators' role in controlling the swimming bias in modulating navigation in porous media by comparing the movement of cells under conditions of increasing agar concentrations (Figures 4A,B). We also included $\Delta cheA1$ and $\Delta cheA4$ mutants that are impaired or null for chemotaxis, respectively (Figures 4A,B; Bible et al., 2008; Mukherjee et al., 2016), and the *rpoN::Km^r* mutant strain that is immotile and lacks flagella (Milcamps et al., 1996). At low agar concentrations (0.2–0.3%), *A. brasilense* cells are swimming through the medium using their polar flagellum,

given the abundance of water under these conditions and previous observation by others (Hall and Krieg, 1983; Moens et al., 1995b; Figure 4). At higher agar concentrations (0.6–0.7%), wild type cells are preferentially swarming using lateral flagella, given that they are observed to move on top of the medium and that these agar concentrations were previously described as optimum for swarming for *A. brasilense* (Hall and Krieg, 1983; Moens et al., 1995b). Navigation of the wild type cells within or on top of the medium at intermediate agar concentrations (0.4%) was minimal, suggesting that both swimming and swarming are limited under these conditions (Figures 4A,B).

Compared to the wild type, the *rpoN::Km^r* mutant did not expand beyond the inoculation point, regardless of agar concentrations, a behavior mimicked by the chemotaxis null

mutants $\Delta cheA4$ and $\Delta cheY7$. The $\Delta cheY4$ mutant had reduced expansion at low agar concentrations (0.2–0.5%) and did not expand beyond the site of inoculation at higher agar concentrations (Figures 4A,B). The $\Delta cheY4$ mutant is non-chemotactic because it seldom reverses swimming direction and this strain also has an elevated frequency of swimming pauses (Mukherjee et al., 2019). We surmise that the limited expansion of the $\Delta cheY4$ cells in media with low agar

concentrations is related to these cells' ability to pause with a high frequency during swimming, which would allow them to escape entrapment into the agar polymers. This swimming bias would not be sufficient to promote movement at higher agar concentrations (0.6–0.7%). The mutants that are impaired but not null for chemotaxis ($\Delta cheA1$, $\Delta cheY1$, and $\Delta cheY6$) displayed either no or only minor defects in navigating within or on top of media of different viscosity. The $\Delta cheA1$ mutant

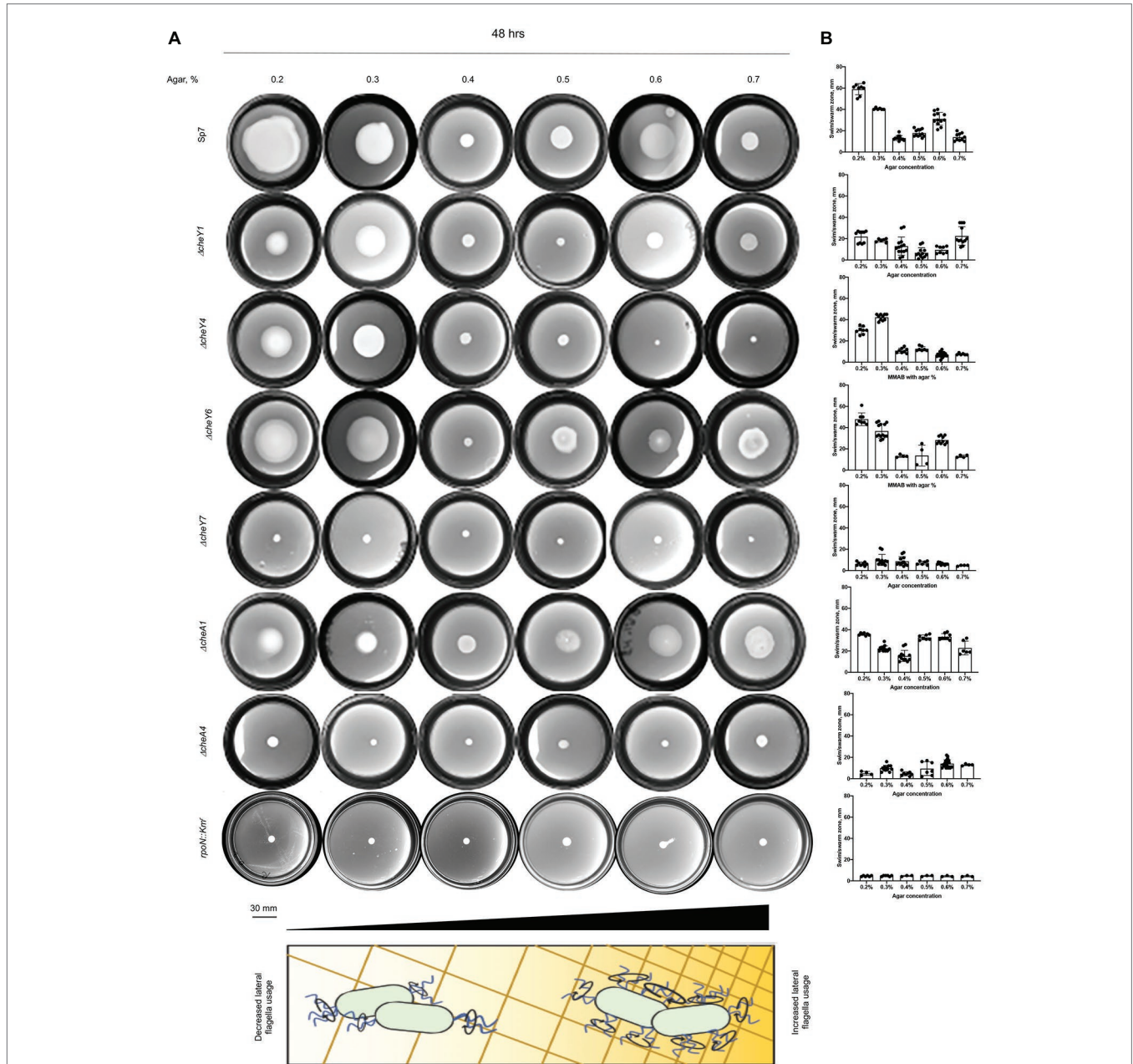
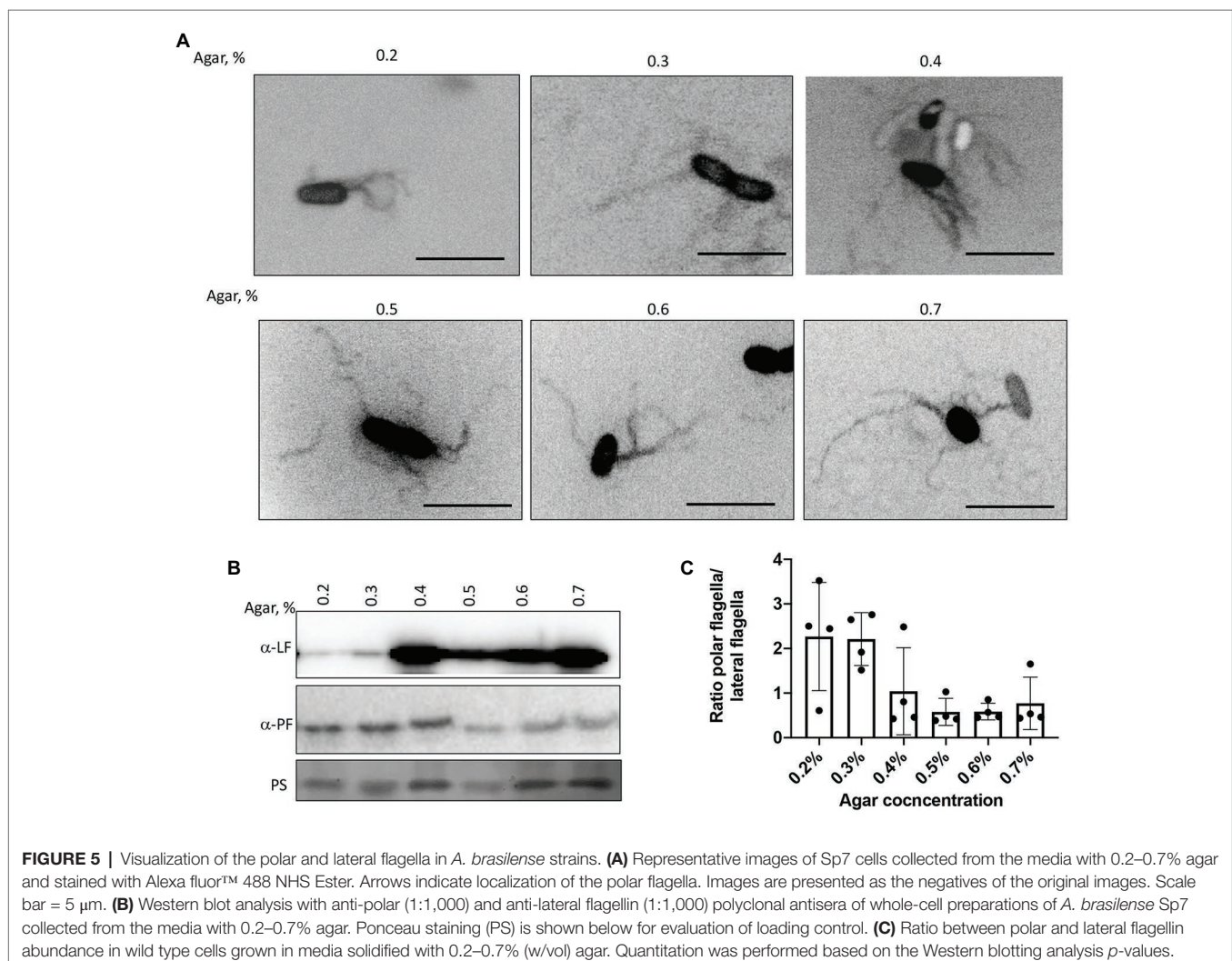


FIGURE 4 | Navigation of *A. brasilense* and its chemotaxis mutant derivatives in soft agar media of varying viscosity. **(A)** Chemotaxis behavior of *A. brasilense* Sp7, $\Delta cheY1$, $\Delta cheY4$, $\Delta cheY6$, $\Delta cheY7$, $\Delta cheA1$, $\Delta cheA4$, and *rpoN::Kmr* strains in the semi-solid medium supplemented with 0.2–0.7% agar. The triangle at the bottom and the scheme represents increasing concentrations of agar. **(B)** Quantitation of the swimming/swarming ring diameters. Arrows indicate a significantly higher swimming/swarming diameter of the colonies in the mutant strains than Sp7. Student *t*-test was used to determine significance between Sp7 and mutants. **p* < 0.05, ***p* < 0.01, ****p* < 0.005, and *****p* < 0.001. All studies were done in three biological replicates.

had a marginally increased expansion through media at the highest agar concentration tested (Figures 4A,B). Together, these data indicate that chemotaxis is essential for the ability of cells to navigate media of varying viscosity, including across surfaces by swarming. Chemical gradients are produced by metabolism as cells move through the agar media and grow indicating that the existence of a gradient is sufficient to trigger an expansion in viscous media by either swimming or swarming. The data presented here confirm the hypothesis that $\Delta cheY1$ and $\Delta cheY6$ mutants are functionally linked to $\Delta cheA1$, while $\Delta cheY4$ and $\Delta cheY7$ cells are related to $\Delta cheA4$ mediated signaling.

We next confirmed the type of motility employed by the cells under these conditions by visualizing the wild type strain's flagellation when inoculated in semi-soft media at different agar concentrations (Figure 5A). At 48 h post-inoculation, both polar and lateral flagella were visible regardless of agar concentration (Figure 5A). Lateral flagella are not produced constitutively in contrast to the polar flagellum in *A. brasilense*. However, we observed some wild type cells with lateral flagella, even at low viscosity [0.2% (v/v) of agar]. This suggests that conditions in the soft agar plates are heterogeneous and do

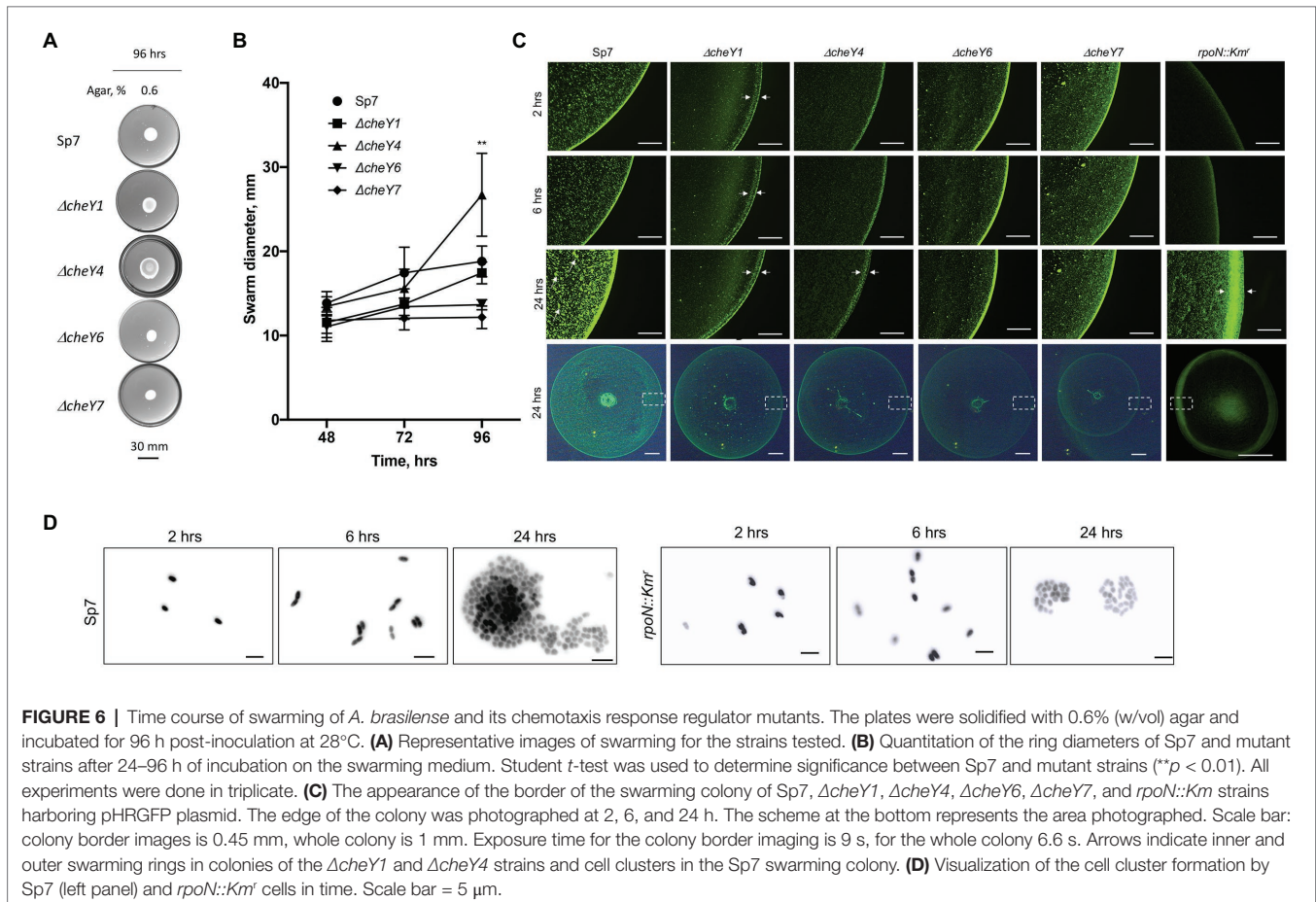
not perfectly replicate a single motility type. To confirm these observations, we used polyclonal antisera raised against the polar and lateral flagellins and Western blots (Figures 5B,C). As expected, the anti-polar flagellin antisera recognized a single band at ~100 kDa in cells grown at various viscosity. The most significant induction of the lateral flagellin production, relative to the polar flagellin production, was observed starting at 0.4% agar in the medium and remained elevated at higher viscosity conditions (Figures 5B,C). Concurrent to these changes, we also observed that cell size distribution varied depending on agar concentrations. The wild type cells were the shortest when incubated in 0.2% agar plates. They tended to increase in size when cells were incubated in media with 0.3–0.6% agar and became shorter at 0.7% agar. However, cells from 0.7% agar were longer than cells at 0.2% agar (Supplementary Figure 1). The longer cell sizes roughly match the induction of lateral flagellin production under these conditions, suggesting that cell elongation is concomitant with swarming. These findings are consistent with similar differentiation observed in other species (Kim et al., 2003; Skerker and Laub, 2004; Little et al., 2019).



To determine whether the defects were due to lack of swarming vs. delayed swarming, we also compared $\Delta cheY1$, $\Delta cheY4$, $\Delta cheY6$, and $\Delta cheY7$ mutants with the wild type Sp7 strain for swarming over time. We performed the experiments using MMAB medium solidified with 0.6% noble agar and supplemented with Tween-20, corresponding to conditions that permit robust swarming (Figures 6A,B). Compared to the wild type strain, all mutants had reduced swarming over the 96 h time-course experiment except for the $\Delta cheY4$ strain, which increased swarming at 96 h post-inoculation, following a reduced swarming at other time points (Figures 6A,B). The $\Delta cheY4$ strain also appeared to expand into a larger swarm colony than the wild type strain under these conditions. This result indicates that the $\Delta cheY4$ strain, but not the other strains, is delayed in inducing swarming. Collectively, the data suggest that CheY7 is essential for swarming and that CheY4 is necessary for timely swarming.

The surface of swarming colonies also differ between the strains: the swarming colonies of the wild type, the $\Delta cheY6$, and $\Delta cheY7$ mutants had a homogenous surface appearance while the swarming colonies of the $\Delta cheY1$ and $\Delta cheY4$ displayed a thick front edge and a thinner, less dense inner region, suggesting that the reduced swarming of the strains could be caused by different group behaviors within the swarming colony. To further characterize cells' behavior in swarming

colonies, we next labeled cells with a constitutively expressed GFP from a plasmid (Ramos et al., 2002) and inoculated these on top of a swarming agar pad. We used fluorescent microscopy to observe cellular behavior at the initiation of swarming (first 24 h). Under these conditions, the wild type cells appeared to organize into a dense edge at the expanding front of the swarming colony, while cells formed clusters that grew in density over time behind this front (Figure 6C). A thick edge was seen in the $rpoN::Km^r$ mutant that is non-motile and non-flagellated, suggesting that it corresponds to non-motile cells. Still, the density of cells under these conditions did not change behind this front in the mutant, suggesting that motility is required for this organization (Figure 6C). A major difference was evident between the wild type swarming colony and the $cheY$ mutants: no increasing clustering of cells behind the expanding front was observed in any of the mutants (Figure 6C). This observation indicates that the organization of cells as high-density clusters is required for the ability of a swarming colony to expand on a surface. Given the differences in the $cheY$ and $rpoN::Km^r$ mutant strains, the lack of cellular clustering suggests that swimming motility, a polar flagellum able to reverse, change swimming speed, and pause is essential for this behavior. A second difference was that the $\Delta cheY1$ and $\Delta cheY4$ swarming colony's edge was thicker and diffuse compared to that of the wild type or the other mutants. In contrast,



the $\Delta cheY6$ and $\Delta cheY7$ swarm colonies had a uniform and bright expanding edge that did not thicken over time compared to that of the wild type (Figure 6C). When compared to the behavior of the $rpoN::Km^r$ mutant under these conditions, the $\Delta cheY6$ and $\Delta cheY7$ mutant strains may differ in the timing or proportion of cells losing motility that produces the edge of the swarm under these conditions compared to the $\Delta cheY1$ and $\Delta cheY4$ or wild type swarming colonies (Figure 5C). In all *cheY* and the $rpoN::Km^r$ mutants, cell density was noticeably reduced behind this expanding edge. Consistent with the results above, the size of the swarming colonies at 24 h was similar in all the mutants, except for the $\Delta cheY7$ and the $rpoN::Km^r$ mutants, which produced significantly smaller swarms at 24 h post-inoculation under these conditions (Figure 6C). These results suggest that swarming requires that cells be able to form high-density clusters behind a sharp and dense expanding edge that may be composed of non-motile cells. When observed under high magnification (Figure 6D), cells behind the expanding edge appeared to be organized as growing clusters that adopt a three-dimensional organization in the wild type but not in the immotile $rpoN::Km^r$ mutant, suggesting a role of motility for these clusters (Figure 6D). Given that some of the mutants are still able of chemotaxis (CheY1, CheY6) while others are chemotaxis null (CheY4 and CheY6), these results indicate that chemotaxis *per se* is not required for the formation of these clusters but that functional CheY response regulators are essential for this behavior. Together, our data indicate that chemotaxis underlies the expansion of a swarming colony across media of high viscosity and that motility and functional CheYs, but not chemotaxis *per se*, is required for initial cell-cell interactions and clustering within a swarming colony.

Lateral Flagella Are Produced in All but the $\Delta cheY7$ Mutant

Swarming depends on the production of lateral flagella, prompting us to analyze lateral flagella and flagellin production in the chemotaxis mutants (Figures 7A–C). Flagella staining revealed that lateral flagella were abundant at 24 h post-inoculation in the $\Delta cheY1$, $\Delta cheY4$, and $\Delta cheY6$ mutants, less abundant in the $\Delta cheY7$ mutant and, as expected, absent in the $rpoN::Km^r$ mutant (Figures 7A–C). This suggests that the reduced swarming of the *cheY* mutant strains is not due to the inability to induce lateral flagella production. Next, we used polyclonal antisera raised against the lateral flagellin and Western blots to compare lateral flagellin production in the wild type and the chemotaxis mutant strains with the immotile $rpoN::Km^r$ strain as a negative control (Figures 7B,C). As expected, the anti-lateral flagellin antisera recognized a single band, at ~45 kDa, in all strains, except the $rpoN::Km^r$ mutant. Relative to the wild type Sp7 strain, the $\Delta cheY7$ mutant, but not the other strains, had a significantly lower abundance of lateral flagellin, consistent with our observations from flagella staining (Figure 7A). Thus, the inability of strain $\Delta cheY7$ to swarm is likely related to its reduced lateral flagellin production. The other mutants' reduced swarming is not related to defects in the production of lateral flagella or lateral flagellin.

Compared to the wild type, swarming cells of the $\Delta cheY1$, $\Delta cheY4$, $\Delta cheY6$, and $\Delta cheY7$ and the $rpoN::Km^r$ mutant strains were shorter in length compared to the wild type, consistent with their defective swarming (Figure 7D). Together, these data suggest that productive swarming requires lateral flagellin production and cell elongation in *A. brasilense* and that cells with defective swarming also display defective cell elongation. These observations are consistent with observations by others that productive swarming requires cell elongation and increased lateral flagella production (Little et al., 2019). Together, the data indicate that the chemotaxis mutants studied here can induce lateral flagella and differentiate into swarmer cells, albeit at different levels. The reduced (or lack of) swarming of these mutants is not due to an inability to produce cellular structures required for swarming.

Functional CheY Homologs, but Not Chemotaxis, Contribute to Attachment to Abiotic and Root Surfaces

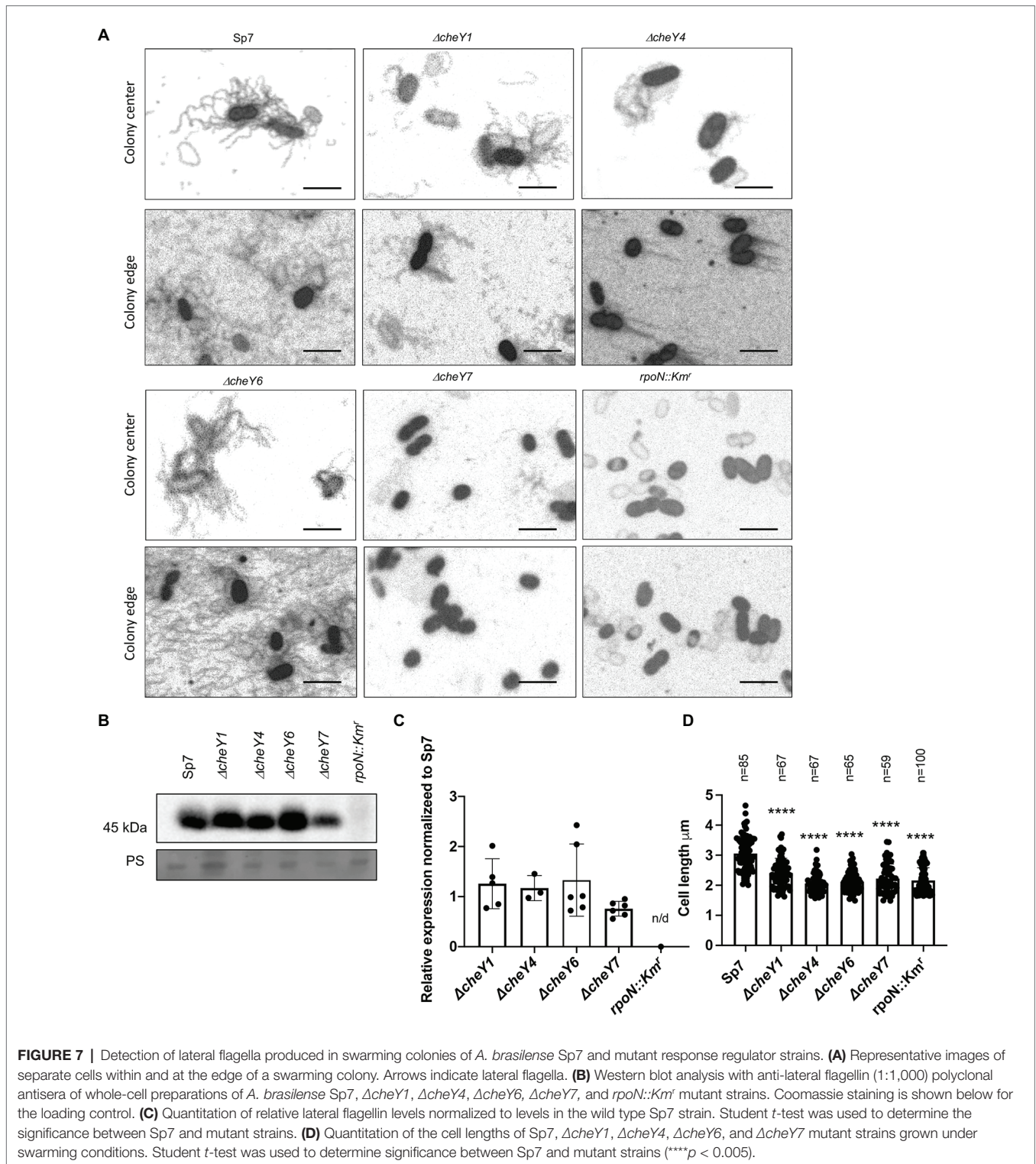
Given the previously reported role of the polar flagellum in an initial attachment to a surface (about 2 h; Michiels et al., 1991), we next compared CheY homologs for contribution to attachment to abiotic surfaces. We used a wild type Sp7, $\Delta cheY1$, $\Delta cheY4$, $\Delta cheY6$, and $\Delta cheY7$ strains harboring pHRGFP plasmid (Ramos et al., 2002) to monitor attachment to poly-lysine coated glass slides over a 2-h incubation period. Relative to the wild type, the $\Delta cheY1$ cells attached better while the $\Delta cheY4$, $\Delta cheY6$, and to a lesser extent, $\Delta cheY7$ cells, attached significantly less to abiotic surfaces (Figures 8A,B).

A similar pattern of attachment to sterile wheat roots was observed (Figure 8C), with the $\Delta cheY1$ attaching better to wheat roots within a 2-h incubation compared to the wild type or the other mutant strains.

We also monitored formation of biofilms *in vitro* and detected major differences at 96 h post-inoculation. The $\Delta cheY1$ strain formed more biofilms relative to the wild type strain, and the $\Delta cheY4$ and $\Delta cheY6$ strains formed less biofilm. The $\Delta cheY7$ mutant did not display any significant defect in biofilm formation relative to the wild type (Figure 8D). The data obtained here in abiotic surface and root attachment and biofilm formation are in good agreement and indicate that CheY homologs are required for attachment and biofilm formation. However, the differences between the strains are unrelated to their steady-state swimming bias or their chemotaxis abilities. These results suggest that functional chemotaxis, which is absent in strains lacking CheY4 or CheY7 and present in strains lacking CheY1 and CheY6, is not directly implicated in these behaviors. The results also imply that the control of the polar flagellum rotation by CheY homologs triggers distinct attachment behaviors.

DISCUSSION

Here, we show that the four CheY homologs that regulate the polar flagellum rotational bias in *A. brasilense* and differentially alter chemotaxis and aerotaxis responses have distinct effects on



swarming and attachment to surfaces. Specifically, we show that chemotaxis signaling, mediated by the CheY homologs' activity studied here, is required for the ability of colonies to expand within or atop media of varying viscosity, likely in response to gradients generated by cell metabolism during this movement. This is similar to findings reported for the role of chemotaxis

in mediating expansion of swarming colonies in gradients in other dually flagellated bacteria such as *Vibrio parahaemolyticus* (Sar et al., 1990), *Vibrio alginolyticus* (Kojima et al., 2007), and *Rhodospirillum centenum* (Jiang et al., 1997). However, this role for chemotaxis in promoting the expansion of swarming colonies is not shared by other species, which increased production of

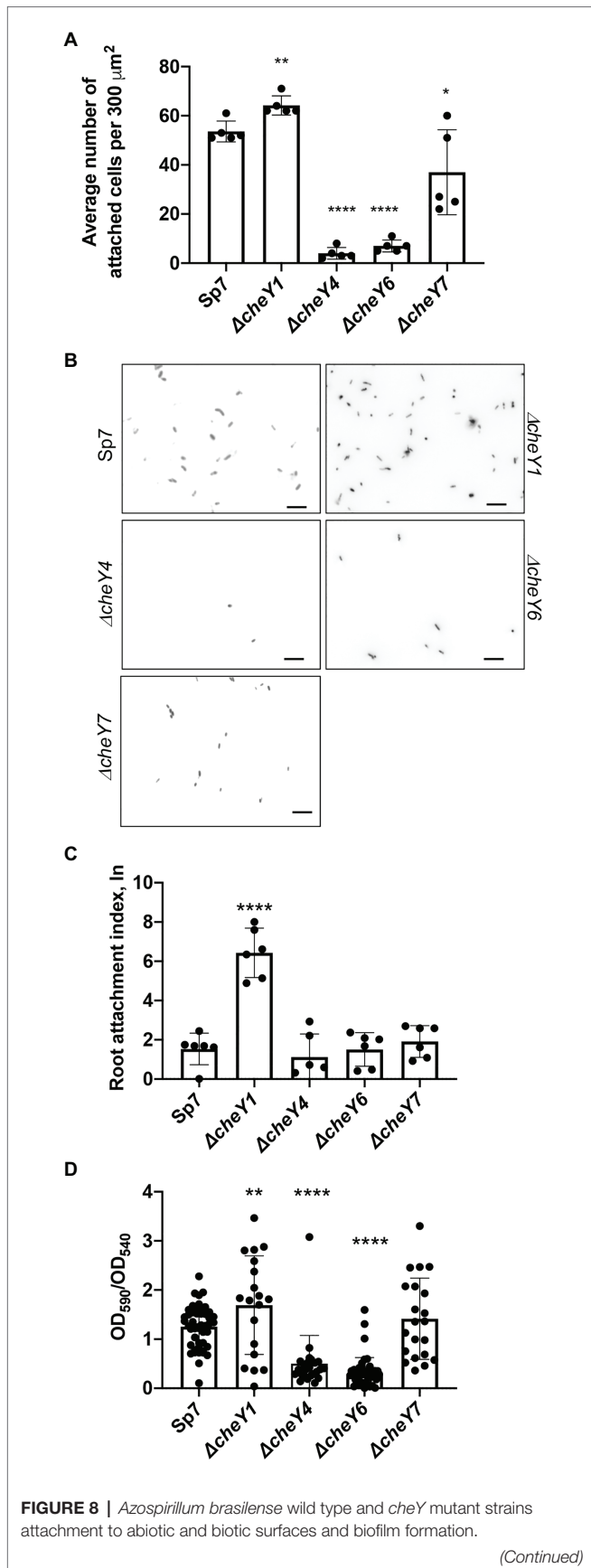


FIGURE 8 | (A) Quantitation of cell attachment of the Sp7, ΔcheY1 , ΔcheY4 , ΔcheY6 , and ΔcheY7 strains labeled carrying pHRGFP, which constitutively expresses green fluorescent protein (GFP), to glass slides coated with poly-lysine (* $p < 0.05$, ** $p < 0.01$, and **** $p < 0.001$). (B) Examples of images of the Sp7, ΔcheY1 , ΔcheY4 , ΔcheY6 , and ΔcheY7 cells attached to poly-lysine coated glass slides. Scale bar is 10 μm . (C) Quantitation of cell attachment of the Sp7, ΔcheY1 , ΔcheY4 , ΔcheY6 , and ΔcheY7 strains carrying pHRGFP, which constitutively expresses GFP, to sterile wheat roots. Student *t*-test was used to determine significance between Sp7 and mutant strains (**** $p < 0.005$). (D) Quantitative biofilm formation by Sp7, ΔcheY1 , ΔcheY4 , ΔcheY6 , and ΔcheY7 cells formed in 96 h. Student *t*-test was used to determine significance between Sp7 and mutant strains (** $p < 0.01$ and **** $p < 0.005$).

a single type of flagella during swarming, such as *E. coli* (Burkart et al., 1998) or *Bacillus subtilis* (Kearns and Losick, 2003).

Functional CheYs appear required for the organization of cells in clusters that formed behind the moving edge of a swarming colony in *A. brasilense*. The cell clusters observed in the wild type are reduced or absent in the *cheY* mutant strains. Our data suggest that the formation of these clusters contributes to productive swarming in *A. brasilense* since swarming is diminished or absent in the chemotaxis *cheY* mutants, despite their ability to induce lateral flagella production. However, we recognize that our experimental design was limited and that additional mutants and higher-resolution imaging are needed to conclude on their role during swarming expansion. We note that these clusters could resemble groups of cells, named rafts or packs that have been seen in other bacterial species (Copeland and Weibel, 2009; Partridge and Harshey, 2013). In *E. coli* and *B. subtilis*, these rafts move together, form and reform continuously with collisions leading to realignment of cells along their long axis and the observation of swirling motions (Turner et al., 2010). The role of chemotaxis in mediating cell-to-cell interactions has been previously demonstrated in several motile bacteria, including *A. brasilense* (Bible et al., 2008; Alexandre, 2015), but the exact mechanism(s) are not known. In *E. coli* (Burkart et al., 1998) and other species that use a single type of flagellum for swimming and swarming, such as *B. subtilis* (Kearns and Losick, 2003) and *P. aeruginosa* (Overhage et al., 2008), a basal level of changes in swimming direction (tumble) triggered by chemotaxis signaling is required for proficient swarming, though the tumbling rate is significantly lower than that observed for free-swimming cells (Partridge et al., 2019). This behavior is thought to promote side-by-side cell alignments and coordinated movement of groups of cells within packs as the swarming colony advances (Partridge et al., 2019, 2020). The lateral flagella that power swarming in *A. brasilense* are structurally different from the polar flagellum, and these differences extend to flagellar motors composed of distinct proteins. We have no evidence that the lateral flagella reverse swimming direction during swarming in *A. brasilense* or that the CheY homologs studied here interact with lateral flagella motors. We only have experimental evidence these CheY homologs control the polar flagellum rotational bias (Mukherjee et al., 2019). The polar flagellum is constitutively produced and persists in swarming cells in *A. brasilense* (Hall and Krieg, 1983; Borisov et al., 2009), but its role is unclear. We have not measured motility and

analyzed the motility bias directly from swarming cells. Therefore, how the CheY homologs exert their effects on swarming through control of the polar flagellum rotational bias remains to be elucidated.

The advancing edge of the *A. brasilense* swarming colony suggested it organized as a densely front of cells, similar to the swarm monolayers described in other bacterial species (Partridge and Harshey, 2013). The swarm colony's moving edge appears to include non-motile cells, similar to observations made in other bacterial species (Copeland and Weibel, 2009). The CheY homologs had different effects on this organization: strains lacking CheY6 and CheY7 formed a sharp front of densely packed cells, while strains lacking CheY1 and CheY4 formed a less defined front. These strains have different swimming biases and chemotaxis abilities. These differences could suggest that the role of CheY in this organization is independent from their role during chemotaxis. A similar observation was previously described in *E. coli* (Burkart et al., 1998). Together, the data suggest that CheY homologs are somehow required for motility loss and the formation of an advancing edge of a swarming colony in *A. brasilense*.

Our data also indicate that both CheY4 and CheY7 play a major role in induction of lateral flagella production and initiation of swarming, with CheY7 being essential for this function and CheY4 being required for timely induction of swarming upon surface contact. This is in contrast to the chemotaxis-independent induction of swarmer cell differentiation in *R. centenum* (Jiang et al., 1997) and *V. parahaemolyticus* (Sar et al., 1990), which also possess two types of flagellar systems and somewhat similar to the role of chemotaxis in inducing swarmer cell differentiation in *E. coli* and other species using a single flagellar system for swimming and swarming. $\Delta cheY4$ and $\Delta cheY7$ cells are both non-chemotactic suggesting that chemotaxis is required for induction of lateral flagella production and swarming motility. This effect is unlikely to be directly related to the rotational bias of the polar flagellum since CheY6 and CheY4 provoke similar rates of swimming reversals of the polar flagellum but a strain lacking CheY6 shows a greatest defect in swarming differentiation (as observed by changes in cell lengths) compared to a strain lacking CheY4, which swarms at high rates after a prolonged delay. In *A. brasilense*, production of the lateral flagellin (Laf1) which is the major component of the lateral flagella and required for swarming is induced when rotation of the polar flagellum is hindered (Moens et al., 1996). An extracytoplasmic factor (ECF) sigma homolog was recently shown to be at the top of a regulatory cascade that negatively regulates lateral flagellin biogenesis in *A. brasilense* (Dubey et al., 2020). These findings, together, suggest that some form of envelope stress may be a triggering signal for induction of lateral flagella in *A. brasilense*. If this is the case, then our findings suggest that CheY7 and CheY4 play essential roles in this signaling event.

Similar to their role in swarming, our results indicate that the *A. brasilense* CheY homologs, but not chemotaxis, mediate short-term attachment to abiotic surfaces and wheat roots, with these effects leading to similar changes in initial

biofilm formation. These effects did not correlate with chemotaxis ability or polar flagellum motor bias. We note that all chemotaxis mutants have lower swimming speed compared to the wild type in the absence of a gradient but they can transiently increase swimming speed in response to attractants, with the exception of a strain lacking CheY1 which is locked at low speeds (Bible et al., 2012; Mukherjee et al., 2016, 2019). A lower swimming speed for this strain would increase its residence time in proximity to surfaces, which could promote enhanced adhesion for this mutant relative to the other strains. Several lines of experimental evidence indicate that chemotaxis signaling regulates non-chemotaxis functions in *A. brasilense*, though the mechanism(s) are not known (Bible et al., 2008; Gullett et al., 2017; Ganusova et al., 2021). It is thus also possible that the *cheY* mutants have different cell surface properties which would modulate their ability to adhere to surfaces.

Collectively, the data obtained here suggest that multiple CheY homologs not only fine tune the rotational bias of flagellar motors and chemotaxis but also promote behaviors that depend on motility such as swarming and attachment to surfaces.

DATA AVAILABILITY STATEMENT

The original contributions presented in the study are included in the article/**Supplementary Material**, further inquiries can be directed to the corresponding author.

AUTHOR CONTRIBUTIONS

EG designed and conducted the experiments, analyzed the data, and wrote the manuscript. LV and TM designed and conducted the experiments, and analyzed the data. GA designed the experiments, analyzed the data, and wrote the manuscript. All authors contributed to the article and approved the submitted version.

FUNDING

This research was supported by a National Science Foundation grant NSF-MCB 1715185 and NSF-MCB 1855066 (to GA). Any opinions, findings, conclusions, or recommendations expressed in this material are those of the authors and do not necessarily reflect the views of the National Science Foundation.

SUPPLEMENTARY MATERIAL

The Supplementary Material for this article can be found online at: <https://www.frontiersin.org/articles/10.3389/fmicb.2021.664826/full#supplementary-material>

Supplementary Figure 1 | Distribution of the cell sizes of *Azospirillum brasilense* Sp7 grown in the media solidified with 0.2–0.7% (w/vol) agar.

REFERENCES

- Alexandre, G. (2015). Chemotaxis control of transient cell aggregation. *J. Bacteriol.* 197, 3230–3237. doi: 10.1128/JB.00121-15
- Alexandre, G., Greer, S. E., and Zhulin, I. B. (2000). Energy taxis is the dominant behavior in *Azospirillum brasilense*. *J. Bacteriol.* 182, 6042–6048. doi: 10.1128/JB.182.21.6042-6048.2000
- Alexandre, G., Rohr, R., and Bally, R. (1999). A phase variant of *Azospirillum lipoferum* lacks a polar flagellum and constitutively expresses mechanosensing lateral flagella. *Appl. Environ. Microbiol.* 65:4701. doi: 10.1128/AEM.65.10.4701-4704.1999
- Alves, L. P., Almeida, A. T., Cruz, L. M., Pedrosa, F. O., de Souza, E. M., Chubatsu, L. S., et al. (2017). A simple and efficient method for poly-3-hydroxybutyrate quantification in diazotrophic bacteria within 5 minutes using flow cytometry. *Br. J. Med. Biol. Res.* 50:e5492. doi: 10.1590/1414-431X20165492
- Arruebarrena Di Palma, A., Pereyra, C. M., Moreno Ramirez, L., Xiqui Vázquez, M. L., Baca, B. E., Pereyra, M. A., et al. (2013). Denitrification-derived nitric oxide modulates biofilm formation in *Azospirillum brasilense*. *FEMS Microbiol. Lett.* 338, 77–85. doi: 10.1111/1574-6968.12030
- Belyakov, A., Burygin, G., Arbatsky, N., Shashkov, A., Selivanov, N., Matora, L., et al. (2012). Identification of an O-linked repetitive glycan chain of the polar flagellum flagellin of *Azospirillum brasilense* Sp7. *Carbohydr. Res.* 361C, 127–132. doi: 10.1016/j.carres.2012.08.019
- Berleman, J. E., and Bauer, C. E. (2005). Involvement of a Che-like signal transduction cascade in regulating cyst cell development in *Rhodospirillum centenum*. *Mol. Microbiol.* 56, 1457–1466. doi: 10.1111/j.1365-2958.2005.04646.x
- Bible, A., Russell, M. H., and Alexandre, G. (2012). The *Azospirillum brasilense* Che1 chemotaxis pathway controls swimming velocity, which affects transient cell-to-cell clumping. *J. Bacteriol.* 194, 3343–3355. doi: 10.1128/JB.00310-12
- Bible, A. N., Stephens, B. B., Ortega, D. R., Xie, Z., and Alexandre, G. (2008). Function of a chemotaxis-like signal transduction pathway in modulating motility, cell clumping, and cell length in the alphaproteobacterium *Azospirillum brasilense*. *J. Bacteriol.* 190:6365. doi: 10.1128/JB.00734-08
- Borisov, I. V., Schelud'ko, A. V., Petrova, L. P., and Katsy, E. I. (2009). Changes in *Azospirillum brasilense* motility and the effect of wheat seedling exudates. *Microbiol. Res.* 164, 578–587. doi: 10.1016/j.micres.2007.07.003
- Burkart, M., Toguchi, A., and Harshey, R. M. (1998). The chemotaxis system, but not chemotaxis, is essential for swarming motility in *Escherichia coli*. *Proc. Natl. Acad. Sci. U. S. A.* 95, 2568–2573. doi: 10.1073/pnas.95.5.2568
- Chawla, R., Gupta, R., Lele, T. P., and Lele, P. P. (2020). A Skeptic's guide to bacterial mechanosensing. *J. Mol. Biol.* 432, 523–533. doi: 10.1016/j.jmb.2019.09.004
- Copeland, M., and Weibel, D. (2009). Bacterial swarming: a model system for studying dynamic self-assembly. *Soft Matter* 5, 1174–1187. doi: 10.1039/b812146j
- Croes, C., Moens, S., Bastelaere, E., Vanderleyden, J., and Michiels, K. (1993). Polar flagellum mediates *Azospirillum brasilense* adsorption to wheat roots. *Microbiology* 139, 2261–2269. doi: 10.1099/00221287-139-9-2261
- de Oliveira Pinheiro, R., Boddey, L. H., James, E. K., Sprent, J. I., and Boddey, R. M. (2002). Adsorption and anchoring of *Azospirillum* strains to roots of wheat seedlings. *Plant Soil* 246, 151–166. doi: 10.1023/A:1020645203084
- Dubey, A. P., Pandey, P., Singh, V. S., Mishra, M. N., Singh, S., Mishra, R., et al. (2020). An ECF41 family σ factor controls motility and biogenesis of lateral flagella in *Azospirillum brasilense* sp245. *J. Bacteriol.* 202, e00231–e00220. doi: 10.1128/JB.00231-20
- Edwards, A. N., Siuti, P., Bible, A. N., Alexandre, G., Retterer, S. T., Doktycz, M. J., et al. (2011). Characterization of cell surface and extracellular matrix remodeling of *Azospirillum brasilense* chemotaxis-like 1 signal transduction pathway mutants by atomic force microscopy. *FEMS Microbiol. Lett.* 314, 131–139. doi: 10.1111/j.1574-6968.2010.02156.x
- Ferré, A., De La Mora, J., Ballado, T., Camarena, L., and Dreyfus, G. (2004). Biochemical study of multiple CheY response regulators of the chemotactic pathway of *Rhodobacter sphaeroides*. *J. Bacteriol.* 186, 5172–5177. doi: 10.1128/JB.186.15.5172-5177.2004
- Figurski, D. H., and Helinski, D. R. (1979). Replication of an origin-containing derivative of plasmid RK2 dependent on a plasmid function provided in trans. *Proc. Natl. Acad. Sci. U. S. A.* 76, 1648–1652. doi: 10.1073/pnas.76.4.1648
- Ganusova, E. E., Vo, L. T., Abraham, P. E., O'Neal Yoder, L., Hettich, R. L., and Alexandre, G. (2021). The *Azospirillum brasilense* core chemotaxis proteins CheA1 and CheA4 link chemotaxis signaling with nitrogen metabolism. *mSystems* 6, e01354–e01420. doi: 10.1128/mSystems.01354-20
- Gordon, V. D., and Wang, L. (2019). Bacterial mechanosensing: the force will be with you, always. *J. Cell Sci.* 132:jcs227694. doi: 10.1242/jcs.227694
- Greer-Phillips, S. E., Stephens, B. B., and Alexandre, G. (2004). An energy taxis transducer promotes root colonization by *Azospirillum brasilense*. *J. Bacteriol.* 186, 6595–6604. doi: 10.1128/JB.186.19.6595-6604.2004
- Gullett, J. M., Bible, A., and Alexandre, G. (2017). Distinct domains of CheA confer unique functions in chemotaxis and cell length in *Azospirillum brasilense* Sp7. *J. Bacteriol.* 199, e00189–e00117. doi: 10.1128/JB.00189-17
- Gunsolus, I. L., Hu, D., Mihai, C., Lohse, S. E., Lee, C. S., Torelli, M. D., et al. (2014). Facile method to stain the bacterial cell surface for super-resolution fluorescence microscopy. *Analyst* 139, 3174–3178. doi: 10.1039/C4AN00574K
- Guttenplan, S. B., and Kearns, D. B. (2013). Regulation of flagellar motility during biofilm formation. *FEMS Microbiol. Rev.* 37, 849–871. doi: 10.1111/1574-6976.12018
- Hall, P. G., and Krieg, N. R. (1983). Swarming of *Azospirillum brasilense* on solid media. *Can. J. Microbiol.* 29, 1592–1594. doi: 10.1139/m83-243
- Hallez, R., Letesson, J.-J., Vandenhoute, J., and De Bolle, X. (2007). Gateway-based destination vectors for functional analyses of bacterial ORFomes: application to the Min system in *Brucella abortus*. *Appl. Environ. Microbiol.* 73, 1375–1379. doi: 10.1128/AEM.01873-06
- Hauwaerts, D., Alexandre, G., Das, S. K., Vanderleyden, J., and Zhulin, I. B. (2002). A major chemotaxis gene cluster in *Azospirillum brasilense* and relationships between chemotaxis operons in α -proteobacteria. *FEMS Microbiol. Lett.* 208, 61–67. doi: 10.1111/j.1574-6968.2002.tb11061.x
- Huang, Z., Wang, Y.-H., Zhu, H.-Z., Andrianova, E. P., Jiang, C.-Y., Li, D., et al. (2019). Cross talk between chemosensory pathways that modulate chemotaxis and biofilm formation. *mBio* 10, e02876–e02818. doi: 10.1128/mBio.02876-18
- Hyakutake, A., Homma, M., Austin, M. J., Boin, M. A., Häse, C. C., and Kawagishi, I. (2005). Only one of the five CheY homologs in *Vibrio cholerae* directly switches flagellar rotation. *J. Bacteriol.* 187, 8403–8410. doi: 10.1128/JB.187.24.8403-8410.2005
- Jiang, Z. Y., Gest, H., and Bauer, C. E. (1997). Chemosensory and photosensory perception in purple photosynthetic bacteria utilize common signal transduction components. *J. Bacteriol.* 179, 5720–5727. doi: 10.1128/JB.179.18.5720-5727.1997
- Kearns, D. B., and Losick, R. (2003). Swarming motility in undomesticated *Bacillus subtilis*. *Mol. Microbiol.* 49, 581–590. doi: 10.1046/j.1365-2958.2003.03584.x
- Keen, N. T., Tamaki, S., Kobayashi, D., and Trollinger, D. (1988). Improved broad-host-range plasmids for DNA cloning in gram-negative bacteria. *Gene* 70, 191–197. doi: 10.1016/0378-1119(88)90117-5
- Kim, W., Killam, T., Sood, V., and Surette, M. G. (2003). Swarm-cell differentiation in *Salmonella enterica* serovar typhimurium results in elevated resistance to multiple antibiotics. *J. Bacteriol.* 185, 3111–3117. doi: 10.1128/JB.185.10.3111-3117.2003
- Kojima, M., Kubo, R., Yakushi, T., Homma, M., and Kawagishi, I. (2007). The bidirectional polar and unidirectional lateral flagellar motors of *Vibrio alginolyticus* are controlled by a single CheY species. *Mol. Microbiol.* 64, 57–67. doi: 10.1111/j.1365-2958.2007.05623.x
- Laganenka, L., Colin, R., and Sourjik, V. (2016). Chemotaxis towards autoinducer 2 mediates autoaggregation in *Escherichia coli*. *Nat. Commun.* 7:12984. doi: 10.1038/ncomms12984
- Levit, M. N., and Stock, J. B. (2002). Receptor methylation controls the magnitude of stimulus-response coupling in bacterial chemotaxis. *J. Biol. Chem.* 277, 36760–36765. doi: 10.1074/jbc.M204325200
- Little, K., Austerman, J., Zheng, J., and Gibbs, K. A. (2019). Cell shape and population migration are distinct steps of *Proteus mirabilis* swarming that are decoupled on high-percentage agar. *J. Bacteriol.* 201, e00726–e00718. doi: 10.1128/JB.00726-18
- Michiels, K. W., Croes, C. L., and Vanderleyden, J. (1991). Two different modes of attachment of *Azospirillum brasilense* Sp7 to wheat roots. *Microbiology* 137, 2241–2246. doi: 10.1099/00221287-137-9-2241
- Milcamps, A., Van Dommelen, A., Stigter, J., Vanderleyden, J., and de Bruijn, F. J. (1996). The *Azospirillum brasilense* *rpoN* gene is involved in nitrogen fixation,

- nitrate assimilation, ammonium uptake, and flagellar biosynthesis. *Can. J. Microbiol.* 42, 467–478. doi: 10.1139/m96-064
- Miller, L. D., Yost, C. K., Hynes, M. F., and Alexandre, G. (2007). The major chemotaxis gene cluster of *Rhizobium leguminosarum* bv. viciae is essential for competitive nodulation. *Mol. Microbiol.* 63, 348–362. doi: 10.1111/j.1365-2958.2006.05515.x
- Moens, S., Michiels, K., Keijers, V., Van Leuven, F., and Vanderleyden, J. (1995a). Cloning, sequencing, and phenotypic analysis of *laf1*, encoding the flagellin of the lateral flagella of *Azospirillum brasilense* Sp7. *J. Bacteriol.* 177, 5419–5426. doi: 10.1128/jb.177.19.5419-5426.1995
- Moens, S., Michiels, K., and Vanderleyden, J. (1995b). Glycosylation of the flagellin of the polar flagellum of *Azospirillum brasilense*, a Gram-negative nitrogen-fixing bacterium. *Microbiology* 141, 2651–2657. doi: 10.1099/13500872-141-10-2651
- Moens, S., Schloter, M., and Vanderleyden, J. (1996). Expression of the structural gene, *laf1*, encoding the flagellin of the lateral flagella in *Azospirillum brasilense* Sp7. *J. Bacteriol.* 178, 5017–5019. doi: 10.1128/jb.178.16.5017-5019.1996
- Mukherjee, T., Elmas, M., Vo, L., Alexiades, V., Hong, T., and Alexandre, G. (2019). Multiple CheY homologs control swimming reversals and transient pauses in *Azospirillum brasilense*. *Biophys. J.* 116, 1527–1537. doi: 10.1016/j.bpj.2019.03.006
- Mukherjee, T., Kumar, D., Burriss, N., Xie, Z., and Alexandre, G. (2016). *Azospirillum brasilense* chemotaxis depends on two signaling pathways regulating distinct motility parameters. *J. Bacteriol.* 198, 1764–1772. doi: 10.1128/JB.00020-16
- O'Neal, L., Gullett, J. M., Aksenova, A., Hubler, A., Briegel, A., Ortega, D., et al. (2019). Distinct chemotaxis protein paralogs assemble into chemoreceptor signaling arrays to coordinate signaling output. *mBio* 10, e01757–e01719. doi: 10.1128/mBio.01757-19
- O'Neal, L., Vo, L., and Alexandre, G. (2020). Specific root exudate compounds sensed by dedicated chemoreceptors shape *Azospirillum brasilense* chemotaxis in the rhizosphere. *Appl. Environ. Microbiol.* 86, e01026–e01020. doi: 10.1128/AEM.01026-20
- Overhage, J., Bains, M., Brazas, M. D., and Hancock, R. E. W. (2008). Swarming of *Pseudomonas aeruginosa* is a complex adaptation leading to increased production of virulence factors and antibiotic resistance. *J. Bacteriol.* 190:2671. doi: 10.1128/JB.01659-07
- Partridge, J. D., and Harshey, R. M. (2013). Swarming: flexible roaming plans. *J. Bacteriol.* 195, 909–918. doi: 10.1128/JB.02063-12
- Partridge, J. D., Nhu, N. T. Q., Dufour, Y. S., and Harshey, R. M. (2019). *Escherichia coli* remodels the chemotaxis pathway for swarming. *mBio* 10, e00316–e00319. doi: 10.1128/mBio.00316-19
- Partridge, J. D., Nhu, N. T. Q., Dufour, Y. S., and Harshey, R. M. (2020). Tumble suppression is a conserved feature of swarming motility. *mBio* 11, e01189–e01120. doi: 10.1128/mBio.01189-20
- Pitzer, J. E., Sultan, S. Z., Hayakawa, Y., Hobbs, G., Miller, M. R., and Motaleb, M. A. (2011). Analysis of the *Borrelia burgdorferi* cyclic-di-GMP-binding protein PlzA reveals a role in motility and virulence. *Infect. Immun.* 79, 1815–1825. doi: 10.1128/IAI.00075-11
- Porter, S. L., Wadhams, G. H., Martin, A. C., Byles, E. D., Lancaster, D. E., and Armitage, J. P. (2006). The CheYs of *Rhodospirillum rubrum*. *J. Biol. Chem.* 281, 32694–32704. doi: 10.1074/jbc.M606016200
- Ramos, H. J. O., Roncato-Maccari, L. D. B., Souza, E. M., Soares-Ramos, J. R. L., Hungria, M., and Pedrosa, F. O. (2002). Monitoring *Azospirillum*-wheat interactions using the *gfp* and *gusA* genes constitutively expressed from a new broad-host range vector. *J. Biotechnol.* 97, 243–252. doi: 10.1016/S0168-1656(02)00108-6
- Sar, N., McCarter, L., Simon, M., and Silverman, M. (1990). Chemotactic control of the two flagellar systems of *Vibrio parahaemolyticus*. *J. Bacteriol.* 172, 334–341. doi: 10.1128/JB.172.1.334-341.1990
- Schmitt, R. (2002). Sinorhizobial chemotaxis: a departure from the enterobacterial paradigm. *Microbiology* 148, 627–631. doi: 10.1099/00221287-148-3-627
- Simon, R., Priefer, U., and Pühler, A. (1983). A broad host range mobilization system for in vivo genetic engineering: transposon mutagenesis in gram negative bacteria. *Bio/Technology* 1, 784–791. doi: 10.1038/nbt1183-784
- Skerker, J. M., and Laub, M. T. (2004). Cell-cycle progression and the generation of asymmetry in *Caulobacter crescentus*. *Nat. Rev. Microbiol.* 2, 325–337. doi: 10.1038/nrmicro864
- Steenhoudt, O., and Vanderleyden, J. (2000). *Azospirillum*, a free-living nitrogen-fixing bacterium closely associated with grasses: genetic, biochemical and ecological aspects. *FEMS Microbiol. Rev.* 24, 487–506. doi: 10.1111/j.1574-6976.2000.tb00552.x
- Stephens, B. B., Loar, S. N., and Alexandre, G. (2006). Role of CheB and CheR in the complex chemotactic and aerotactic pathway of *Azospirillum brasilense*. *J. Bacteriol.* 188, 4759–4768. doi: 10.1128/JB.00267-06
- Turner, L., Zhang, R., Darnton, N. C., and Berg, H. C. (2010). Visualization of flagella during bacterial swarming. *J. Bacteriol.* 192:3259. doi: 10.1128/JB.00083-10
- Viruega-Góngora, V. I., Acatitla-Jácome, I. S., Reyes-Carmona, S. R., Baca, B. E., and Ramírez-Mata, A. (2020). Spatio-temporal formation of biofilms and extracellular matrix analysis in *Azospirillum brasilense*. *FEMS Microbiol. Lett.* 367:fnaa037. doi: 10.1093/femsle/fnaa037
- Wu, L., Cui, Y., Hong, Y., and Chen, S. (2011). A CheR/CheB fusion protein is involved in cyst cell development and chemotaxis in *Azospirillum brasilense* Sp7. *Microbiol. Res.* 166, 606–617. doi: 10.1016/j.micres.2010.12.001
- Wu, Z., He, R., Zhang, R., and Yuan, J. (2020). Swarming motility without flagellar motor switching by reversal of swimming direction in *E. coli*. *Front. Microbiol.* 11:1042. doi: 10.3389/fmicb.2020.01042
- Zamudio, M., and Bastarrachea, F. (1994). Adhesiveness and root hair deformation capacity of *Azospirillum* strains for wheat seedlings. *Soil Biol. Biochem.* 26, 791–797. doi: 10.1016/0038-0717(94)90275-5
- Zhulin, I. B., and Armitage, J. P. (1992). The role of taxis in the ecology of *Azospirillum*. *Symbiosis* 13, 199–206.
- Zhulin, I. B., and Armitage, J. P. (1993). Motility, chemokinesis, and methylation-independent chemotaxis in *Azospirillum brasilense*. *J. Bacteriol.* 175, 952–958. doi: 10.1128/JB.175.4.952-958.1993
- Zhulin, I. B., Bespalov, V. A., Johnson, M. S., and Taylor, B. L. (1996). Oxygen taxis and proton motive force in *Azospirillum brasilense*. *J. Bacteriol.* 178, 5199–5204. doi: 10.1128/JB.178.17.5199-5204.1996

Conflict of Interest: The authors declare that the research was conducted in the absence of any commercial or financial relationships that could be considered as a potential conflict of interest.

Copyright © 2021 Ganusova, Vo, Mukherjee and Alexandre. This is an open-access article distributed under the terms of the Creative Commons Attribution License (CC BY). The use, distribution or reproduction in other forums is permitted, provided the original author(s) and the copyright owner(s) are credited and that the original publication in this journal is cited, in accordance with accepted academic practice. No use, distribution or reproduction is permitted which does not comply with these terms.